metals

MDPI

Review

Advanced Self-Passivating Alloys for an Application under Extreme Conditions

Andrey Litnovsky [1,2,*], Felix Klein [1], Xiaoyue Tan [1,3], Janina Ertmer [1,4], Jan W. Coenen [1,5], Christian Linsmeier [1], Jesus Gonzalez-Julian [1], Martin Bram [1], Ivan Povstugar [6], Thomas Morgan [7], Yury M. Gasparyan [2], Alexey Suchkov [8], Diana Bachurina [8], Duc Nguyen-Manh [9], Mark Gilbert [9], Damian Sobieraj [10], Jan S. Wróbel [10], Elena Tejado [11], Jiri Matejicek [12], Henning Zoz [13], Hans Ulrich Benz [13], Pawel Bittner [1] and Anicha Reuban [1]

1 Forschungszentrum Jülich GmbH, Institut für Energie und Klimaforschung, 52425 Jülich, Germany; fe.klein@fz-juelich.de (F.K.); xi.tan@fz-juelich.de (X.T.); janina.ertmer@t-online.de (J.E.); j.w.coenen@fz-juelich.de (J.W.C.); ch.linsmeier@fz-juelich.de (C.L.); j.gonzalez@fz-juelich.de (J.G.-J.); m.bram@fz-juelich.de (M.B.); p.bittner@fz-juelich.de (P.B.); a.reuban@fz-juelich.de (A.R.)
2 Plasma Physics Department, Institute of Laser and Plasmas Technologies, National Research Nuclear University MEPhI, Kashirskoe sh., 31, 115409 Moscow, Russia; ymgasparyan@mephi.ru
3 School of Materials Science and Engineering, Hefei University of Technology, Hefei 230009, China
4 Department of Applied Physics, Ghent University, 9000 Ghent, Belgium
5 Department of Engineering Physics, University of Wisconsin–Madison, Madison, WI 53706, USA
6 Forschungszentrum Jülich GmbH, Zentralinstitut für Engineering, Elektronik und Analytik, 52425 Jülich, Germany; i.povstugar@fz-juelich.de
7 DIFFER—Dutch Institute for Fundamental Energy Research, De Zaale 20, 5612 AJ Eindhoven, The Netherlands; t.w.morgan@differ.nl
8 Department of Materials Science, Institute of Nuclear Physics and Engineering, National Research Nuclear University MEPhI, Kashirskoe sh., 31, 115409 Moscow, Russia; ansuchkov@mephi.ru (A.S.); dmbachurina@mephi.ru (D.B.)
9 CCFE, United Kingdom Atomic Energy Authority, Culham Science Centre, Abingdon OX14 3DB, UK; duc.nguyen@ukaea.uk (D.N.-M.); mark.gilbert@ukaea.uk (M.G.)
10 Faculty of Materials Science and Engineering, Warsaw University of Technology, Wołoska 141, 02-507 Warsaw, Poland; damian.sobieraj.dokt@pw.edu.pl (D.S.); jan.wrobel@pw.edu.pl (J.S.W.)
11 Departamento de Ciencia de Materiales-CIME, Universidad Politécnica de Madrid, C/Profesor Aranguren 3, E28040 Madrid, Spain; elena.tejado@upm.es
12 Institute of Plasma Physics of the Czech Academy of Sciences, Za Slovankou 3, 18200 Praha, Czech Republic; matejicek@ipp.cas.cz
13 Zoz Group, Maltoz-Str., 57482 Wenden, Germany; zoz@zoz.de (H.Z.); benz@zoz.de (H.U.B.)
* Correspondence: a.litnovsky@fz-juelich.de

check for updates

Citation: Litnovsky, A.; Klein, F.; Tan, X.; Ertmer, J.; Coenen, J.W.; Linsmeier, C.; Gonzalez-Julian, J.; Bram, M.; Povstugar, I.; Morgan, T.; et al. Advanced Self-Passivating Alloys for an Application under Extreme Conditions. *Metals* **2021**, *11*, 1255. https://doi.org/10.3390/met11081255

Academic Editor: Jiro Kitagawa

Received: 25 June 2021
Accepted: 23 July 2021
Published: 9 August 2021

Abstract: Self-passivating Metal Alloys with Reduced Thermo-oxidation (SMART) are under development for the primary application as plasma-facing materials for the first wall in a fusion DEMOnstration power plant (DEMO). SMART materials must combine suppressed oxidation in case of an accident and an acceptable plasma performance during the regular operation of the future power plant. Modern SMART materials contain chromium as a passivating element, yttrium as an active element and a tungsten base matrix. An overview of the research and development program on SMART materials is presented and all major areas of the structured R&D are explained. Attaining desired performance under accident and regular plasma conditions are vital elements of an R&D program addressing the viability of the entire concept. An impressive more than 10^4-fold suppression of oxidation, accompanied with more than 40-fold suppression of sublimation of tungsten oxide, was attained during an experimentally reproduced accident event with a duration of 10 days. The sputtering resistance under DEMO-relevant plasma conditions of SMART materials and pure tungsten was identical for conditions corresponding to nearly 20 days of continuous DEMO operation. Fundamental understanding of physics processes undergone in the SMART material is gained via fundamental studies comprising dedicated modeling and experiments. The important role of yttrium, stabilizing the SMART alloy microstructure and improving self-passivating behavior, is under investigation. Activities toward industrial up-scale have begun, comprising the first mechanical alloying with an industrial partner and the sintering of a bulk SMART alloy sample with dimensions

of 100 mm × 100 mm × 7 mm using an industrial facility. These achievements open the way to further expansion of the SMART technology toward its application in fusion and potentially in other renewable energy sources such as concentrated solar power stations.

Keywords: DEMO safety; self-passivating tungsten alloys; fast; suppressed oxidation; erosion resistance

1. Introduction

The safety aspect will play a key role in the design and envisaged operation of future fusion power plants. Obeying stringent safety requirements will become compulsory for, e.g., obtaining the licensing to build a plant. It is expected that the level and stringency of safety requirements for licensing of a power plant will exceed that imposed on the international ITER project [1,2]. At the same time, in the course of an intensive R&D of the DEMOnstration power plant (DEMO), besides the ultimate operational challenge. questioning the use of conventional materials adopted to ITER, a significant safety risk was revealed. In the course of safety assessment undertaken under the European Fusion Development Agreement (EFDA) framework, several severe accident scenarios were assessed by predictive modeling [3]. The study demonstrated, that in the course of a severe accident, where the loss-of-coolant accident (LOCA) was accompanied with air ingress into the vacuum vessel due to e.g., its mechanical damage or destruction, the temperature of the foreseen pure tungsten plasma-facing first wall can rise up to 1000 °C and higher due to nuclear decay heat. In the absence of active cooling, such a temperature is expected to last at the level of 1000 °C for several weeks after the accident despite radiative cooling. Being exposed to the atmosphere, tungsten will oxidize. In the course of exposure to fusion neutrons during the regular plasma operation, tungsten becomes a radioactive material. Tungsten oxide is volatile and therefore an aerosol containing a radioactive oxide WO_3 will be formed and sublimated into the atmosphere. Assuming a total area of the first wall of DEMO of 1000 m^2, which corresponds to the power plant size in the study [3], an estimate was given in [4] of the expected sublimation rate. Depending on the temperature, the sublimation rates may vary between 10 and 150 kg per hour. Assuming an average sublimation rate of 100 kg/h, the entire first wall of the DEMO power plant may become sublimated within approximately one month. The corresponding cumulative activity of mobilized tungsten will exceed 1.8×10^{19} Bq using the data from [5]. Therefore, active sublimation of the radioactive material must be decreased and, if possible, suppressed completely.

In order to address the above-mentioned radiation hazard, Koch and Bolt [6] have introduced the concept of self-passivating tungsten alloys in 2007. This new class of tungsten-based materials must adapt its properties depending on the environment. In the course of regular plasma operation, the lighter alloying elements will be preferentially sputtered by plasma particles. As a result, the remaining, nearly pure tungsten surface will create a shield protecting alloying elements from further sputtering. During a severe accident, the formerly protective pure tungsten layer with a thickness of several nanometers will be inevitably oxidized and sublimated into the atmosphere. Given the minute thickness of such a pure tungsten layer, the total amount of sublimated material ranging from 19 to 190 g becomes nearly negligible when compared to the 60 tons of the pure tungsten first wall. The remaining alloying elements will create their own oxide scale in turn on the surface of the tungsten, protecting tungsten from oxidation and therefore preventing the sublimation of tungsten oxide. The concept of self-passivating systems provides human-independent passive safety which is triggered by the accident event itself–a feature highly desirable for a fusion power plant.

A significant research and development activity is currently underway on self-passivating alloys for fusion power plants, as referred in e.g., dedicated reviews [7–13]. Bulk Self-passivating Metal Alloys with Reduced Thermo-oxidation (SMART) systems are under

development at the Forschungszentrum Jülich GmbH, Germany, jointly with several international partner institutions and teams. The present SMART materials contain tungsten (W), forming the alloy matrix, chromium (Cr) acting as a passivating element, and yttrium (Y), the so-called active element [14–18]. The SMART systems have pioneered the use of yttrium at an appropriate concentration as an active element in the alloy. Yttrium supports and stabilizes the oxidation protection of tungsten provided by chromium.

Since the last overview of the SMART alloy activity published in 2020 [12], progress in research and development of the SMART alloy systems has become so significant and versatile that a new review became necessary. This time, the authors decided to provide the structure of the research along with goals and priorities. These changes are significant, and they are felt to be necessary in order to guide a reader through the review and to present a logical path of the ongoing research.

2. The Structure of Research and Development of SMART Systems

The structure of the R&D on SMART systems is presented in Figure 1. Since the principal feature of SMART systems compared to pure tungsten is their envisaged ability to mitigate oxidation and sublimation of tungsten oxide, the prime focus of initial investigations was on providing the required oxidation resistance. The corresponding review of the most important results is provided in the section "Oxidation performance". Since SMART systems are the envisaged plasma-facing materials, their performance under plasma exposure is the second vital pillar in the feasibility of the entire SMART concept and its applicability in a power plant. The main findings of the studies of plasma interaction with the SMART systems are given in the section "Plasma performance". Attaining oxidation resistance while maintaining an acceptable plasma performance are the compulsory prerequisites for a viable material system for fusion application. The material concept created must be industrially compatible at a commercially competitive level. Important activities in thermo-mechanical qualification are described in the section "Thermo-mechanical qualification". Certainly, progress in none of the mentioned areas is imaginable without dedicated fundamental studies throughout the entire R&D process. A compact and comprehensive overview of key fundamental findings regarding SMART systems is provided in the section "Fundamental research". The final goal of the SMART system development is the application of SMART technology for plasma-facing materials of the first wall in DEMO. Significant activities are initiated toward the production of the DEMO first wall mockup at industrial level. These activities are described in the section "Industrial up-scale". Key results from all areas of R&D are provided in a summary, whereas open questions, challenges and strategies for further progress are presented in the outlook.

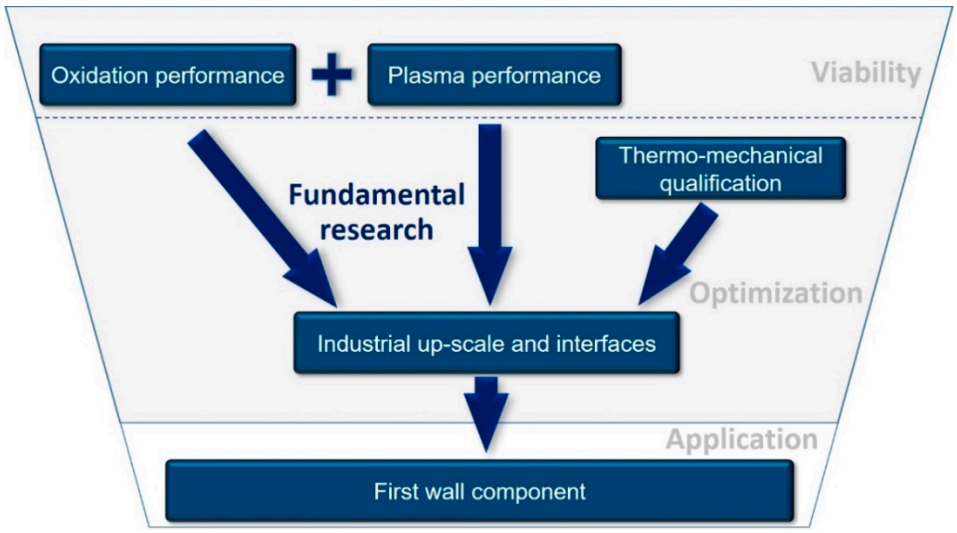

Figure 1. A structure of the research and development program on SMART materials.

3. Oxidation Performance

As mentioned above, attaining oxidation performance is a vital element in the feasibility of application of self-passivating alloys in a fusion power plant. Earlier studies [4,6,19–21] were performed mostly with thin films formed via magnetron deposition. Relatively simple and fast experiments with thin films demonstrated their capability for studying the initial oxidation performance of prospective alloy compositions. The amount of material was just sufficient for obtaining solid data on oxidation performance—a step which saved a lot of effort in comparison to extensive and time-consuming studies on bulk systems.

In all thin film systems, chromium was used as the main alloying element to the base tungsten, whereas various add-on elements, such as silicon and titanium, were used as so-called active alloying elements to increase the performance of an alloy. Although a significant improvement in oxidation resistance was attained at a short timescale for the mentioned thin film systems, none of them was capable of demonstrating the required long-term suppression of oxidation at a scale of several days.

A dramatic improvement came with the introduction of yttrium, with a minute relative concentration in the alloy in the order of 1 atomic percent or less. These studies were pioneered at Forschungszentrum Jülich. Following the available data for corrosion research provided, e.g., in [15–18,22], it was decided to use yttrium as an active element in SMART alloys. Besides its very high affinity for oxygen, which potentially could lead to the cleaning of the SMART system from parasitic oxygen, yttrium features a low volumetric expansion of the oxide, compared to that of pure metal. This volumetric expansion, which is introduced by Pilling and Bedworth [23], can be written as

$$R_{P\text{-}B} = V_{ox}/V_{met}, \quad (1)$$

where V_{met} and V_{ox} are the volumes of a pure metal and its oxide correspondingly.

In order to attain the optimum oxidation resistance, the $R_{P\text{-}B}$ must be within 1 and 2 [23]. Yttrium possesses $R_{P\text{-}B}$ of 1.13, to be compared to $R_{P\text{-}B}$ of pure Cr of 2.01, and that of pure W of 3.39 [23].

These and other arguments were used while choosing yttrium as an active element in SMART systems. Investigations conducted with thin films have revealed clearly superior oxidation resistance of W-Cr-Y SMART alloys as compared to all element combinations studied before [4]. The internal oxidation was suppressed almost completely. Elemental optimization was performed which yielded an optimum concentration of W-11.4Cr-0.6Y, where the numbers are given in weight percent. This combination is used in all subsequently described studies, unless stated otherwise.

The thin W-Cr-Y films, however, were not able to attain the necessary long-term suppression of oxidation due to a lack of alloying material. The corresponding research activities have therefore shifted toward the production of bulk materials. The first step in the production is the mechanical alloying of the source W, Cr and Y powders. This step is treated as virtually inevitable and used by all research groups working on self-passivating alloys worldwide [11,22,24–28]. The following step is the sintering of the alloyed powder. Whereas several research groups prefer to use the hot isostatic pressing (HIP) technique for sintering [24,29], advanced Field-Assisted Sintering Technology (FAST) was used for production of SMART systems. The HIP and FAST feature essentially similar principles and operating parameters. The key difference of FAST is the pulsed or continuous direct current applied to the sample during sintering. Furthermore, sintering is usually done in easy-to-manufacture graphite tools. Possible contamination by carbon due to graphite tools can be easily removed by a simple grinding of sintered samples. In case of SMART materials, grinding of 0.5 mm from each side has been sufficient for removal of carbon contamination. At the same time, a rather complex sealing technology for gas-tight powder encapsulation, as in the case of HIP, is not required. This allows FAST to compact and sinter the sample significantly faster, within minutes, as can be inferred, e.g., from [11,27,30]. The self-passivating samples created using HIP and SMART systems produced using FAST feature essentially the same microstructure and oxidation performance.

The oxidation performance of self-passivating alloys is, in fact, impressive. The corresponding mass change in the course of oxidation in the humid atmosphere of the reference pure sample and SMART systems is presented in Figure 2. As pure tungsten exhibits unattenuated and highly intensive oxidation, the oxidation rate of SMART alloy was measured to be at least 10^4-fold smaller than that of pure tungsten at a timescale of 10 days of continuous exposure. During the exposure, humid air at 70 relative percent humidity was fed at 40 °C to the SMART sample kept at a temperature of 1000 °C, thus representing as-realistic-as-possible conservative conditions assumed for a fusion power plant [30,31].

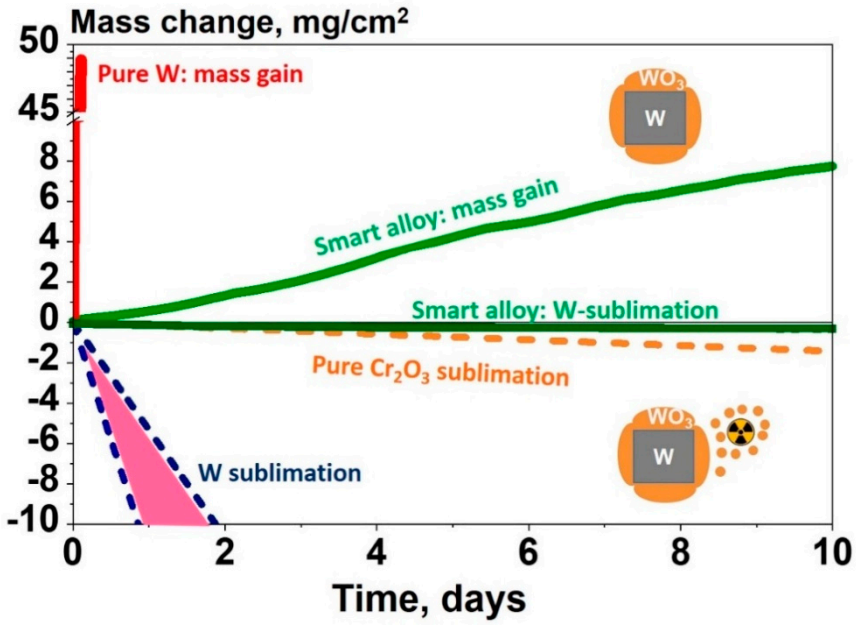

Figure 2. The evolution of mass change, due to oxidation and sublimation depending on exposure time of the SMART alloys, pure tungsten and chromia (Cr_2O_3). Processes of oxidation leading to the mass gain and sublimation leading to the mass loss are shown with schemes in the upper and lower parts of the figure, correspondingly.

The oxidation leads to a mass increase due to growth of tungsten oxide at the surface and in the bulk of the sample, as shown schematically in Figure 2. Oxidation itself, however, does not represent a safety concern directly. It is the sublimation of the oxide which leads to a release of oxidized radioactive materials in case of an accident, as shown in the scheme in Figure 2. Sublimation leads to a decrease of the mass of the sample due to release of a sublimated material.

To the best knowledge of the authors, no direct measurements of tungsten sublimation were available prior to the study on SMART materials published in [30,31]. The measured (solid) and extrapolated from the measurements (dashed) lines represent sublimation rates for pure tungsten (pink area) and chromium oxides (orange dashed line). The inclination of the sublimation curve of SMART material is so low that the curve can hardly be distinguishable from an abscissa line in Figure 2. An impressive 40-fold suppression of sublimation was measured [30,31]. The total area of mixed W-containing oxide after 20 days of continuous oxidation did not exceed 1% [30]. The desired suppression of sublimation was, therefore, demonstrated on SMART W-Cr-Y bulk systems.

4. Plasma Performance

Performance of SMART systems under stationary plasma conditions represents a second vital and necessary aspect in the assessment of an applicability of SMART materials in fusion devices. An introduction of alloying elements in the tungsten matrix was not

expected to result in any improvement of plasma performance of SMART materials. In fact, the similarity of plasma performance in terms of sputtering resistance and deuterium retention was anticipated as a success.

In order to investigate the plasma performance, a series of studies were performed on SMART systems [32–37]. In all these studies performance of SMART alloys was directly compared to that of pure tungsten made by an industrial company using ITER specifications [38,39]. This was made either by placing the SMART samples along with pure W samples on the same holder and by exposing them under identical conditions as realized in linear plasma device PSI-2 in Julich [32–34,37], or by repeating the experiments by keeping the plasma conditions identical for pairs of SMART and pure W samples, as in the experiments in the divertor simulator Magnum-PSI located in the DIFFER institute in Eindhoven [12,36].

During all exposures, the plasma parameters were chosen and controlled as closely as possible to those expected during the regular plasma operation in DEMO. The temperature of all samples was always kept in the range of 590 °C–650 °C [32–37] as expected for the first wall in DEMO [40].

A series of key parameters such as surface recession due to sputtering, mass loss due to sputtering, deuterium retention during exposure, surface morphology and microstructure were monitored using several surface diagnostic techniques. An extensive description of the methods applied can be found, e.g., in [32,33].

Among all plasma conditions studied, exposures in steady-state deuterium plasmas corresponding to the regular operation of DEMO are of prime importance. A summary of these studies performed both in PSI-2 and in Magnum-PSI is provided in [36]. The most important result is shown in Figure 3, as a dependence of mass loss for both SMART materials and pure tungsten on plasma fluence. The energies of deuterium ions were kept at 120 eV, as a conservative estimate for DEMO conditions, whereas the temperature of all samples was kept within 570 °C–650 °C during exposures.

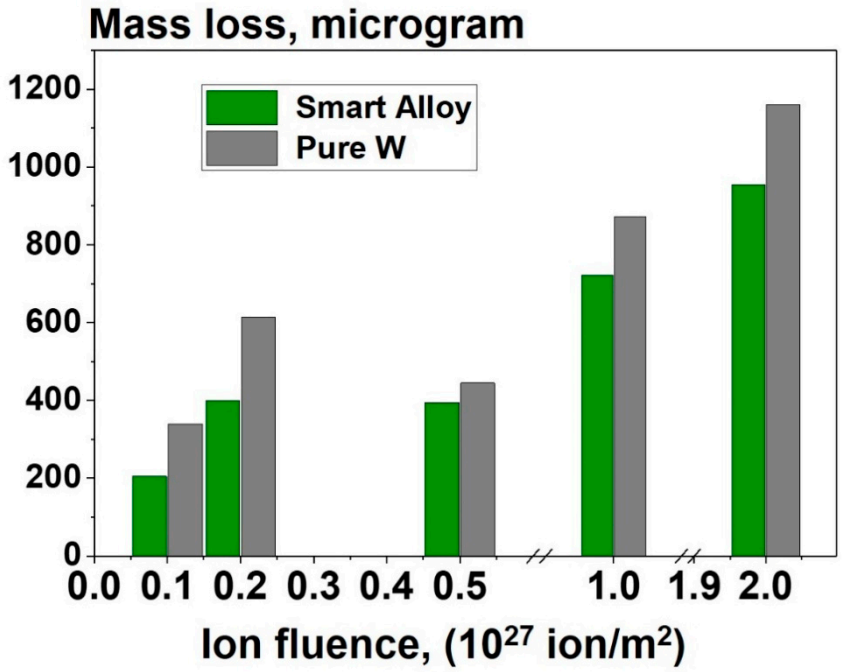

Figure 3. Mass loss due to sputtering erosion of SMART alloys and pure tungsten as a function of plasma fluence.

As can be inferred from Figure 3, the pure tungsten has exhibited the highest mass loss. The surface recession measured, e.g., during experiments at 0.1×10^{27} ion/m^2 and 0.2×10^{27} ion/m^2 was the same for pure W and SMART materials [33]. Given the

same surface recession via sputtering, the observed higher mass loss of tungsten is due to a higher density of this material. Moreover, the detailed depth analyses of exposed samples provided, e.g., in [33] evidenced the existence of the tungsten layer on the surface, protecting the underlying alloy, as expected in the SMART alloy concept. It should be noted that the conservatively estimated daily fluence to the first wall of DEMO using [40,41] corresponds to roughly 0.1×10^{27} ion/m^2 assuming continuous plasma operation. The experiments performed, therefore, correspond at the highest fluence of 2.0×10^{27} ion/m^2 to at least 20 days of a continuous DEMO operation.

Another important result can be inferred from Figure 3: if uniform sputtering of the W-Cr-Y SMART system is assumed and no measurable disadvantageous additional diffusion of Cr to the surface occurs, the expected ratio of sputtered mass of the SMART system as compared to that of pure W is 0.82. Despite experiments at lower fluences which were mostly short-term and, therefore, prone to higher uncertainty, this is exactly the value measured during high fluence exposures. This finding demonstrates the absence of Cr diffusion towards the surface during the regular plasma operation. This result is of high importance, since otherwise an undesirable diffusion of Cr towards the surface during regular plasma operation of the power plant could have led to the exhaustion of the Cr reservoir in the bulk material, needed for passivation of the first wall in case of an accident.

Plasma performance of SMART alloys has been examined, besides the above-mentioned regime, under a number of various plasma conditions, which might exist in DEMO. Among these conditions are, e.g., the limiter phase operation of DEMO [32,36,37] and the potentially possible seeding of DEMO plasmas [34,35]. Under limiter-phase conditions, SMART systems featured enhanced sputtering compared to that of pure tungsten. In case of plasma seeding described in detail in, e.g., [34–36], the sputtering of both pure W and SMART alloys was significant. These important findings, however, mostly address sensitivity studies for future DEMO scenarios. The enhanced sputtering of SMART systems during the limiter operation will likely play an insignificant role in DEMO, mostly because of a drastic difference in duration of limiter phase operation (minutes) to pulse duration (hours) and expected reduced fluxes of just-born plasmas. The necessity and feasibility of seeding scenarios in DEMO is a subject of intensive discussion in the fusion community and experimental findings obtained for seeding scenarios are certainly providing an important critical input into the assessment of seeding feasibility.

The ultimate conceptual merit for the qualification of of SMART technology is, however, the oxidation resistance after plasma exposure. A series of investigations were performed at Forschungszentrum Jülich. First results of oxidation performance studies involving pure tungsten, the former W-Cr-Ti self-passivating systems and the W-Cr-Y SMART alloys are provided in Figure 4. As expected, both self-passivating systems exhibit a less mass increase due to oxidation, compared to that of pure W. It is also obvious that the SMART W-Cr-Y possesses a superior oxidation resistance compared to the formerly developed W-Cr-Ti alloy during a 10 h exposure under oxidizing conditions. At the same time, the slight degradation of the oxidation resistance of the SMART alloy after plasma exposure at the fluence of "only" 0.2×10^{26} ion/m^2 raised a concern about maintaining the oxidation performance after plasma.

In order to investigate factors influencing the oxidation resistance of plasma-exposed SMART samples, a dedicated study was made. It is known, e.g., [36], that the oxidation resistance especially at the beginning of exposure depends strongly on the quality and purity of the sample under investigation. Here, the geometry of samples used for oxidation resistance studies and those for plasma exposures is significantly different. Samples used for oxidation resistance studies shown in Figure 5b have a simple cube geometry and were ground from all sides. Samples for plasma exposure and subsequent oxidation possess a much more complex geometry presented in Figure 5c. Here, only the bright part was directly exposed to plasma, being mounted onto the holder as shown in Figure 5a. For plasma-exposed samples, only a plasma-facing side and its opposite side could be

ground. Grinding of all other surfaces was impossible and hence these samples remain contaminated with impurities from manufacturing during the oxidation studies.

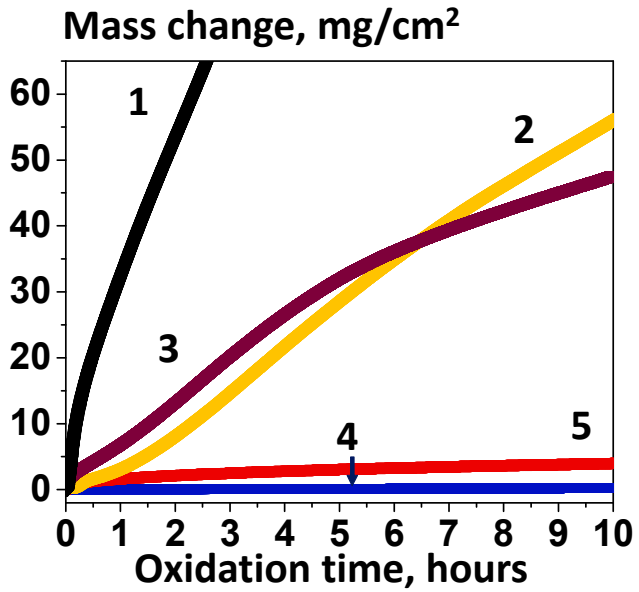

Figure 4. Mass change during the oxidation process: (**1**) for the pure W sample, (**2**) for the reference W-10Cr-2Ti smart alloy [32], (**3**) fir the W-10Cr-2Ti smart alloy exposed in plasma [32], (**4**) for the reference W-11.6Cr-0.6Y smart alloy and (**5**) for the W-11.6Cr-0.6Y smart alloy exposed in plasma. Oxidation took place in an atmosphere consisting at 80 vol.% of Ar + 20 vol.% of O_2 at 1 bar and 1000 °C. Reproduced from [11].

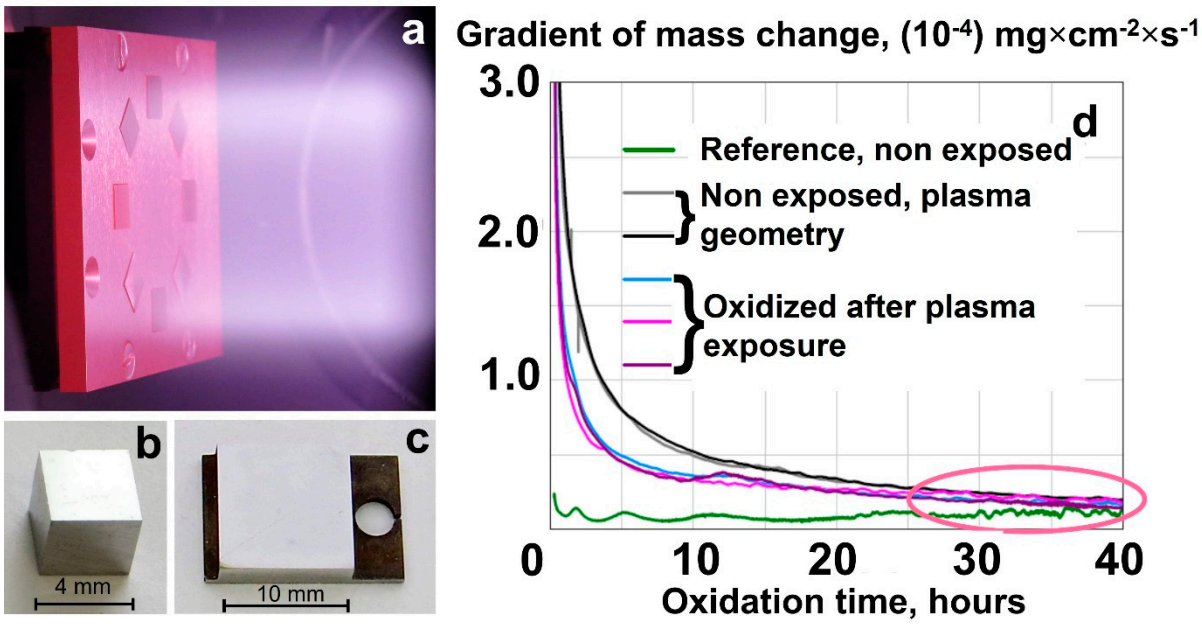

Figure 5. Performance of plasma-exposed SMART alloys: (**a**) photo of a simultaneous exposure of SMART and pure tungsten samples in steady-state deuterium plasma in PSI 2 linear plasma device, (**b**) reference geometry of the samples for the oxidation/sublimation studies, (**c**) plasma geometry of samples and (**d**) the dependence of the mass change rate on oxidation time for the SMART materials of reference and plasma geometry, including plasma-exposed SMART samples oxidized after exposure.

The results of a long-term comparison involving the samples of cube and plasma geometry, exposed under identical oxidizing conditions, are provided in Figure 5d. Here the gradient of mass change, i.e., the rate at which mass changes due to oxidation, is plotted as a function of exposure time. As can be evidenced from Figure 5d, the initial degradation of the oxidation resistance was noticed for both exposed and non-exposed samples of plasma geometry, obviously caused by the initial and unavoidable contamination due to manufacturing of a complex geometry. This effect obviously vanishes after about 25 h of exposure. Contaminants are "burnt" out and the oxidation resistance of all SMART samples is identical, independent of geometry and, most importantly, of plasma exposure.

5. Thermo-Mechanical Qualification

Having succeeded in terms of conceptual feasibility, the next important step was investigation of the basic thermo-mechanical properties of SMART materials. Qualification began with routine hardness measurements made on every sintered ingot. The SMART materials appeared to be rather fragile, having a Vickers hardness $H_{v0.5}$ of about 1100, two–threefold that of pure tungsten. The hardness was measured at room temperature.

The ductile-to-brittle transformation temperature (DBTT) was measured in the course of dedicated investigations. The DBTT of the W-Cr-Y systems was detected to be in the range of 950 °C. The material becomes plastic at temperatures above 1000 °C.

Finally, the thermal conductivity of SMART systems was investigated. The thermal conductivity of SMART systems is about 1/3 of that of tungsten and matches well that of reduced activation ferritic-martensitic (RAFM) steel–a prospective structural material for fusion. The thermal conductivity was measured in the range of RT up to 700 °C, reaching a maximum of about 55 W/(m × K) at ~600 °C and being stable at higher temperatures up to 700 °C. As expected for alloys, the thermal conductivity of SMART systems increases with temperature, whereas for the bulk tungsten it declines.

Current investigations show, in fact, an expected decline in the thermo-mechanical characteristics of SMART systems. At the same time, the thermal and mechanical loads in the area of the prospective application of the SMART systems as the first wall material are rather benign. The relatively thin first wall with a thickness of about 3 mm will be exposed to stationary heat loads in the range of 1–2 MW/m^2 at a temperature of about 650 °C [40,42]. The application of SMART systems in the severely loaded parts such as, e.g., the divertor target is not foreseen.

Nevertheless, despite the fact that there is neither a specific limit nor a forbidding mechanical limitation imposed on the SMART alloy machinability, activities are being undertaken to improve the thermo-mechanical characteristics of SMART systems. The ongoing investigations reveal, e.g., a potential for an improvement via the further optimization of the FAST sintering. Dedicated research [28,43,44] demonstrates, e.g., a significant effect imposed by the sintering current on the microstructure of the alloy. Exploratory studies aiming at further optimizing of the thermo-mechanical properties of SMART systems are an important ongoing research activity.

6. Industrial Up-Scale and Interfaces

The extensive thermo-mechanical characterization described above is intended as a preparation for a further step in the realization of SMART alloy materials for DEMO—an industrial up-scale. An industrial up-scale aims at providing the amount of SMART materials necessary for a power plant (tons). Another important goal of an industrial up-scale is a demonstration of the capability of producing the SMART materials at a necessary size. The first wall armor in DEMO will be castellated by splitting it into a number of smaller-scale segments. This will be made with a view to expected inhomogeneous heat loads. As an example, the largest segment of a beryllium first wall castellation in ITER has a maximum lateral dimension of 50 mm × 50 mm [45,46]. In the course of our industrial up-scale study, we will use these dimensions as a merit, trying to explore the feasibility of larger SMART samples at the same time.

Within the industrial up-scale activity, all processes used for producing the SMART systems have to be transferred and adapted at industry level. Two essential steps in production of SMART materials are mechanical alloying (MA) and FAST.

On the way to industrial up-scale of MA, following the research performed in Jülich [12], the industrial partner Zoz Group was contacted and an R&D collaboration program for MA was established. The industrial partner has a vast experience in the variety of MA applications. The set of industrial W and Cr powders was procured along with Y powder for the first MA attempt. The milling regimes previously explored at Forschungszentrum Jülich [12] were analyzed carefully in a series of joint meetings of FZJ researchers and specialists from the industrial partner.

For the first attempt the Simoloyer® mill developed and manufactured by the industrial partner was used. For the first attempt chromium-containing steel balls were used. The interior of the Simoloyer® was made of stainless steel. Four kilograms of tungsten along with 0.5 kg of Cr powder were used in the first MA at industrial scale. In the course of the milling, periodic sampling of the powder was undertaken after 0.5, 1.5, 6.5, 9.5, 12.5, 18.5, and 21.5 h of milling. All the samples with the powder were delivered to the FZJ where extensive analyses were performed. These analyses comprised X-ray Diffractometry, Energy-Dispersive X-ray Analysis and combustion analysis of carbon impurities.

The results of the MA alloying with an industrial partner evidence a complete alloying of the source powders after 18.5 h of milling already, as compared to 60 h needed in planetary mills available at FZJ. This is probably due to the different way of energy transfer from the balls to the powder particles applied in Simoloyer®. Most of the energy is likely transferred through collisions, in contrast to the collisional-frictional energy transfer, in the planetary mill Retsch 400 MA used in the PowderLab at Forschungszentrum Jülich. Energy transfer in the planetary mills was approached analytically, for instance, in [47]. Despite the intensive collisions of W, Cr and Y powders with the steel balls and walls of the Simoloyer®, the amount of iron was about 2 wt.% after the complete alloying. Such an amount represents presently no safety concern given the limited weight of the SMART first wall compared, e.g., to the weight of stainless steel structural materials in DEMO.

Nevertheless, for future up-scaling studies it was decided to consider the use of hard milling tools in further milling attempts. The next attempt, currently under preparation, will use yttria-stabilized zirconia milling tools.

The second important activity is the industrial up-scale of the FAST technology. Here, the newly available industrial FAST facility Dr Fritsch (Fellbach, Germany) DCP 515 operated at the Institute of Energy and Climate Research, IEK-1: Materials and Processing was used for the first time. The key advantage of this facility is the power, sufficient to fully reproduce the FAST regimes used for sintering of SMART systems at the lab scale. The sintering of the first large-scale SMART sample using an industrial facility was made in late 2020. The operating parameters of Dr. Fritsch DSP 515 are provided in Table 1. The parameters are in fact identical to those used in the lab research and provided in [11,12,31]. The only exception is the application of the direct current in Fritsch DSP 515 instead of pulsed DC current used in the lab.

Table 1. Technological parameters of sintering using the industrial FAST facility of Dr. Fritsch DSP 515.

Parameter	Value
Heating rate, °C/min	200
Applied pressure, MPa	50
Maximum temperature, °C	1460
Holding time at maximum temperature, min	0
DC/Pulsed DC sintering	DC

As a result, the first large SMART alloy sample with dimensions of 100 mm × 100 mm × 7 mm and a total weight of 0.76 kg has been sintered successfully. A sample photo

is provided in Figure 6. The attained density of the first sintered large FAST sample is about 70%, outlining a need in further optimization of the technical parameters of sintering such as protective gas feeding, minimum temperature for gas protection, etc. The new large-scale SMART alloy sample is presently under investigation.

Figure 6. A large-scale bulk SMART alloy sample sintered using the industrial FAST facility.

Apart from up-scaling of the SMART technology, providing robust interfaces to the structural material, RAFM steel is of significant importance. There are several principle approaches to address this topic regarding SMART alloys.

Presently, brazing is deemed as one of the most robust techniques for joining tungsten and steel sub-structures. Brazed parts feature robustness [48,49] along with a possibility of local repair of the small size components, such as the castellated block, in case of damage. Brazing attempts to join the SMART material were undertaken using a pure Cu braze and a Ni interlayer [50,51]. Several advantageous features of the SMART alloy compared to that of pure tungsten were revealed. Having a reactive alloying element, the SMART material shows inter-diffusion into the braze, further strengthening it, unlike pure tungsten which usually exhibits a sharp interface with the braze [52].

Recently, braze experiments have started using the novel titanium–zirconium–beryllium brazing alloy with a composition 48Ti–48Zr–4Be wt.%, rapidly solidified into foil and, hence, amorphous alloys [53,54]. Using such a Cu- and Ni-free alloy opens potentially a way of further reducing the use of Cu, Ni featuring rather high residual activity, in DEMO. The brazed SMART and Rusfer Reduced Activation Ferritic-Martensitic (RAFM) steel blocks in the frame of the thermo-mechanical characterization underwent 100 thermal cycles in the temperature range 300 °C–600 °C. A formation of intermetallic phases was observed at the scale of tens of microns. At the same time, neither cracking nor delamination was detected via scanning electron microscopy after the thermal cycling. An extensive overview of the novel braze systems is provided in [54]. Another potential advantage of brazing is its ability to combine necessary heat treatment of the RAFM steel and brazing in one operation.

Apart from brazing technology, intensive studies have begun in applying FAST for a direct brazing of SMART materials and RAFM. Despite the significant difference in all

major mechanical characteristics including thermal expansion and thermal conductivity coefficient, the FAST technology by itself, featuring local heating at a nanoscale [55,56], may provide conditions for a robust and a very compact interface. Two attempts at joining the RAFM steel (Eurofer) and W-Cr-Y SMART alloy were undertaken. The operating regimes differed in maximum pressure applied and in the time the samples were held at the maximum temperature. A summary of joining attempts is provided in Table 2.

Table 2. Parameters of a first direct joining of SMART materials and RAFM steel (Eurofer) using FAST.

Sample Name	FAST 3125	FAST 3126
Heating rate, °C/min	200	200
Applied pressure, MPa	30	50
Maximum temperature, °C	800	800
Holding at maximum temperature, min	10	60
Sample size, mm^3	10 × 10 × 3	10 × 10 × 3

The sample joined at 50 MPa underwent slow thermal cycling in the range of 300–600 °C. No damage was observed after SEM and TEM observation at nanoscale after seven thermal cycles [57].

Besides the above-mentioned methods, there are a few more joining and interfacing techniques potentially applicable for SMART materials. Among these is additive manufacturing, functionally-graded materials and a low-pressure plasma spray technology. Investigations in these research directions are at an initial exploratory stage.

7. Fundamental Research on SMART Systems

The aim of the R&D on SMART systems is not the sole application of the materials developed in a fusion power plant, but possible expansion of SMART technology for other renewable energy systems working under extreme environments. Such an application is possible only via physics understanding of the processes ongoing in the SMART material in the course of its lifetime. These fundamental studies have been underway since the very beginning of the SMART material concept. In fact, due to these studies, both via modeling and by the dedicated experiments, the sound progress of SMART materials has been attained so far. Fundamental studies of SMART systems address, therefore, physics processes ongoing in SMART alloys both under regular and accident conditions, as well as trying to find answers to questions on stability and the evolution of SMART materials, including exploring the role of every element in the alloy.

While studying oxidation resistance, exploring the impact caused by yttrium on W-Cr-Y system is of crucial importance. A dedicated study is being performed using the first-principles modeling approach [58–61]. The composition stability of the W-Cr-Y system was studied at various temperatures via modeling using the combination of Density Functional Theory (DFT), Cluster Expansion (CE) and Monte-Carlo (MC) methods. At the beginning, DFT database of enthalpies of mixing for a series of ordered binary and ternary structures using Vienna Ab-initio Simulation Package [62,63] was employed to build up the Cluster-Expansion Hamiltonian that includes the interactions between different atoms in the W-Cr-Y system. These Effective Cluster Interactions for two- and three-body clusters were used, in turn, in Monte-Carlo simulations using Alloy Theoretic Automatic Toolkit package [64]. The MC simulations allowed to study the alloy stability for the binary and ternary systems as a function of elemental composition and temperature. The simulations were carried out by quenching alloys from 3000 K down to 100 K with a temperature step of 100 K. Modelling was made for unit cells containing 2000 atoms. The phase stability at a given temperature of considered alloys was specifically analyzed using the enthalpy of mixing derived from the MC simulations [65]. Atomic ordering and segregation within the alloy were analyzed using the MC simulations. In the MC calculation the Warren-Cowley short-range order (SRO) parameters [65–67] were employed, which describe the nature of chemical interactions between different pairs of atoms. Positive values of the SRO

parameter indicate atomic segregation, while negative values suggest the possibility of atomic ordering and, specifically, point out to a possible formation of intermetallic phases.

Modelling shows that in the body-centered cubic (bcc) lattice which is the ground-state structure for both tungsten and chromium, positive values of the SRO are predicted for the W-Cr system. This result means that these elements try to segregate from each other at a wide temperature range in agreement with the experimental phase diagram for this binary system [68]. Alloying yttrium with a solute concentration within 0.5–2.0 at.% into W-Cr alloys reveals strongly positive SRO parameters for both W-Y and Cr-Y pairs over the whole temperature range. In other words, yttrium tends to segregate from both W and from Cr in the alloy at any temperature. SRO values close to zero indicate the possibility of a stable solid solution formation.

Importantly, it is found that in the presence of yttrium, the predicted solid solution temperature is reduced from 1700 K in the binary 70W-30Cr to 1300 K in the ternary 70W-29Cr-1Y. Here the numbers are given in atomic percent corresponding to the experimentally studied alloys with the elemental composition W-11.6 wt.% Cr-0.6 wt.% Y. Modeling studies show that yttrium tries to stabilize the formation of the W-Cr solid solution at lower temperature than that expected for a pure binary system. A dedicated theoretical study is provided in [58].

A comparative study of alloying with titanium, which has a similar ground-state hexagonal close-packed (hcp) structure as yttrium, shows essentially no effect of Ti on changing segregation temperature between W and Cr. The origin of the difference between 70W-29Cr-1Y and 70W-29Cr-1Ti is that the SRO between W and Ti is negative meaning that there is a strong chemical bonding between these two elements in contrast to the positive SRO behavior between W and Y. Therefore, the chances are greatest of finding Y in between the grains. Here, Y can effectively suppress the re-crystallization. Besides suppression of undesirable recrystallization and stabilization of W-Cr solid solution at a lower temperature, the analysis of chemical affinity of yttrium reveals the third potential effect of this active element. Yttrium is likely to bind oxygen in the bulk of SMART material, enabling a cleaner path for Cr for the formation of a protective chromia coating and the reduction of internal oxidation. This "cleaning" action of yttrium is a subject of intensive investigation.

Dedicated studies using atom probe tomography [31,69] have confirmed the segregation of yttrium toward the boundary of W-Cr grains and preferential formation of yttrium-containing oxides. These findings will be summarized in a dedicated paper in the near future.

It is also crucially important to investigate in conclusive detail the process of oxide scale growth. In case of a preferential oxide scale growth toward the bulk of SMART material, the oxide formed, having increased volume, would introduce an additional non-desirable stress at the interface of the SMART alloy system and the protecting layer. This would lead to instability and cracking of the protective oxide. If, on the contrary, the oxide scale grows toward the oxidizing atmosphere out of the substrate, the oxide scale is free to expand, and no destructive stresses are expected. Here, further important knowledge on oxidation resistance has been gained via fine dedicated experiments using oxidation in an atmosphere of oxygen isotope ^{18}O. In studies described in detail in [70], several exposures were made, including one using the ^{18}O. This oxygen isotope was used as a marker to investigate the direction of the oxide scale growth. The dedicated investigations show non-ambiguously that the oxidation is a bidirectional process accompanied by the slower penetration of oxygen inside the SMART material along with a faster diffusion of chromium and subsequent oxidation outside the bulk of SMART system. The resulting gross process is the oxygen scale growth towards the oxidizing atmosphere out of the substrate–a desirable result of extreme importance for the SMART material concept.

Regarding the plasma performance, an important combined experimental and modeling study was performed and reported, e.g., [36,37]. The dedicated modeling was performed using SDTRIMSP code [71] in order to address the measured sputtering of the

SMART material in deuterium plasmas. The study revealed a predominant sputtering action caused by oxygen, a parasitic impurity in the PSI 2 linear plasma device. The estimated amount of oxygen required for an explanation of experimental sputtering rates was estimated to be 0.23% which corresponds well with measurements performed in PSI-2 [36]. This, at first glance, secondary result is in fact of crucial importance since the parasitic oxygen content originating from, e.g., micro-leaks is expected for water-cooled plasma-facing materials in future superconductive fusion devices including DEMO [72,73]. Detection of these microleaks is extremely difficult [74,75] and in situ repair of damaged components is hardly possible. Therefore, the parasitic and dominating sputtering via oxygen is expected to be a common issue. Important knowledge of sputtering by intentionally introduced so-called seeding gases was obtained and presented in, e.g., [34,35]. Here, an important note on the feasibility of seeding and on allowable amount of seeded impurities must be evaluated in future.

8. Summary

In this paper we have reviewed the research and development program on self-passivating SMART materials in the Forschungszentrum Jülich and partner institutions. SMART materials are presently envisaged as prospective risk-mitigation materials for a future fusion power plant.

In the course of the paper the structured R&D program was presented and subsequently each key element of the R&D was described in detail. The viability studies of the SMART materials were performed in order to assess the physics applicability of the concept to DEMO environment. These studies comprised two major constituents: SMART alloy had to demonstrate its performance under accident conditions, as well as during a regular plasma operation.

In the simulated accident conditions, comprising an as-realistic-as-possible scenario of a loss-of-coolant accident with air ingress, the SMART materials featured at least 10^4-fold suppression of oxidation accompanied with at least 40-fold suppression of oxide sublimation, as compared with performance of pure tungsten. The suppressed oxidation and sublimation are guaranteed for at least 20 days after the accident. After such a long exposure, the surface analyses revealed less than 1% percent of the surface area of oxidized SMART material, occupied with mixed W-Y oxide, not a pure WO_3.

At the same time, the sputtering resistance of SMART materials to pure deuterium stationary plasma was investigated in a series of dedicated experiments. The sputtering resistance was expected to be identical to that of pure tungsten for the fluence of up to 2×10^{27} ion/m^2 which corresponds to about 20 days of continuous plasma operation of DEMO. Importantly, the long-term performance of plasma-exposed samples under subsequent accident conditions, did not change as compared to that of unexposed samples.

Important knowledge has been obtained on the mechanical properties of SMART systems. These advanced materials feature presently a rather high hardness of $H_{v0.5}$ ~1100 at room temperature and an average thermal conductivity of about 50 W/(m $\times$ K) at 650 °C. While treated as non-critical presently, there is extensive effort on improvement of these characteristics.

Having finalized the viability studies and attained the optimized technology at the laboratory scale, the main focus is being shifted toward industrial up-scale. Mechanical alloying has been already started with an industrial partner and the first bulk SMART material sample with dimensions of 100 mm $\times$ 100 mm $\times$ 7 mm has been sintered using an industrial device with field-assisted sintering technology.

The design and technology efforts rest on a solid fundamental research basis, providing a crucial input in the physics understanding of SMART materials. The recent fundamental studies comprising first-principles modeling supported with atom probe tomography measurements tend to support the hypothesis of the crucial role of yttrium on reducing recrystallization, on suppression of internal oxidation and on support of chromium transport, necessary for a formation of the thin and dense protective layer.

Crucial knowledge has been obtained via dedicated fundamental studies on oxide formation using the oxidation in an ^{18}O isotope-containing atmosphere. It has been shown non-ambiguously that the protective chromia oxide scale grows towards the oxidizing environment, out of the SMART substrate, thus alleviating and mitigating stresses and maintaining the necessary adhesion. Modeling of plasma performance performed using the SDTRIMSP code has revealed an important role of parasitic impurities in sputtering of both SMART materials and pure tungsten, an issue relevant for DEMO.

9. Outlook

Certainly, there are several open questions to be resolved and knowledge to be expanded. Presently, significant efforts are concentrated on attaining industrial-scale first wall solutions using the SMART materials. The technology must be established with the production of the flat-tile prototype, a first wall mockup for DEMO.

Knowledge of plasma performance of both pure tungsten and SMART alloys provides an important information on plasma compatibility of plasma-facing materials in a fusion power plant. The implementation of these results into DEMO R&D will likely lead to further optimization of the plasma scenarios including a tuning of seeding species and their allowable concentrations.

Our knowledge on the physics effects introduced by the passivating and especially active elements has to be further expanded. This is necessary in order to obtain the full picture of the processes ongoing in SMART materials, on the role of each element in the alloy and for the further study of prospective active and passivating materials. This knowledge is vital for an envisaged expansion of the SMART technology toward non-fusion applications under an extreme environment for future renewable energy sources: concentrated solar power receivers and high-temperature infrastructure components, such as modern heat-exchangers.

Author Contributions: A.L.: conceptualization, writing—original draft preparation, methodology, investigation, formal analysis, conceptualization, funding acquisition and project administration; F.K., X.T., J.E.: conceptualization, investigation, formal analysis, methodology, writing—review and editing; J.W.C. and C.L.: review and editing, funding acquisition and project administration, writing—review and editing; J.G.-J. and M.B.: investigation, funding acquisition, resources, writing—review and editing; I.P., M.G., D.N.-M., J.S.W., Y.M.G., A.S., D.B., D.S., H.U.B., T.M., E.T., J.M.: investigation, methodology, formal analysis, writing—review and editing; H.Z.: formal analysis, resources, writing—review and editing; P.B. and A.R.: investigation, writing—review and editing; All authors have read and agreed to the published version of the manuscript.

Funding: Part of this work has been carried out within the framework of the EUROFusion Consortium and has received funding from the Euratom research and training programme 2014–2018 and 2019–2020 under grant Agreement No. 633053. The views and opinions expressed herein do not necessarily reflect those of the European Commission. The work at Warsaw University of Technology has been carried out as a part of an international project co-financed from the funds of the program of the Polish Minister of Science and Higher Education entitled "PMW" in 2019; Agreement No. 5018/H2020-Euratom/2020/2. Research activities at the CCFE were supported by the RCUK Energy Programme, grant number EP/T012250/1. Collaboration research activities between Forschungszentrum Jülich and Hefei University of Technology were supported by the National Natural Science Foundation of China, grant number 52020105014 and the Natural Science Foundation of Anhui Province, China, grant number 201904b11020034. Investigations at MEPhI were supported by the Russian Science Foundation, grant number 17-72-20191. Reported studies were in part financially supported by the Helmholtz Graduate School for Energy and Climate Research (HITEC) at Forschungszentrum Jülich.

Data Availability Statement: Not applicable.

Conflicts of Interest: The authors declare no conflict of interest.

References

1. Perrault, D. Safety issues to be taken into account in designing future nuclear fusion facilities. *Fusion Eng. Des.* **2016**, *109–111*, 1733–1738. [CrossRef]
2. Van Dorsselaere, J.P.; Perrault, D.; Barrachin, M.; Bentaïb, A.; Gensdarmes, F.; Haeck, W.; Pouvreau, S.; Salat, E.; Séropian, C.; Vendel, J. Progress of IRSN R&D on ITER Safety Assessment. *J. Fusion Energy* **2011**, *31*, 405–410. [CrossRef]
3. Maisonnier, D.; Cook, I.; Sardain, P.; Andreani, R.; Di Pace, L.; Forrest, R.; Giancarli, L.; Hermsmeyer, S.; Norajitra, P.; Taylor, N.; et al. *A Conceptual Study of Commercial Fusion Power Plants*; Final Report of the European Fusion Power Plant Conceptual Study (PPCS); EFDA(05)-27/4.10; European Fusion Development Agreement (EFDA): Garching, Germany, 2005; Volume 1, pp. 1–38.
4. Wegener, T.; Klein, F.; Litnovsky, A.; Rasinski, M.; Brinkmann, J.; Koch, F.; Linsmeier, C. Development of yttrium-containing self-passivating tungsten alloys for future fusion power plants. *Nucl. Mater. Energy* **2016**, *9*, 394–398. [CrossRef]
5. Gilbert, M.R.; Sublet, J.C. *Handbook of Activation, Transmutation, and Radiation Damage Properties of the Elements Simulated Using FISPACT-II & TENDL-2015 for Magnetic Fusion Plants*; Culham: Abingdon, UK, 2016.
6. Koch, F.; Bolt, H. Self passivating W-based alloys as plasma facing material for nuclear fusion. *Phys. Scr.* **2007**, *T128*, 100–105. [CrossRef]
7. Linsmeier, C.; Rieth, M.; Aktaa, J.; Chikada, T.; Hoffmann, A.; Houben, A.; Kurishita, H.; Jin, X.Z.; Li, M.; Litnovsky, A.; et al. Development of advanced high heat flux and plasma-facing materials. *Nucl. Fusion* **2017**, *57*, 092007. [CrossRef]
8. Litnovsky, A.; Wegener, T.; Klein, F.; Linsmeier, C.; Rasinski, M.; Kreter, A.; Unterberg, B.; Coenen, J.; Du, H.; Mayer, J.; et al. Smart tungsten alloys as a material for the first wall of a future fusion power plant. *Nucl. Fusion* **2017**, *57*, 066020. [CrossRef]
9. Litnovsky, A.; Wegener, T.; Klein, F.; Linsmeier, C.; Rasinski, M.; Kreter, A.; Tan, X.; Schmitz, J.; Mao, Y.; Coenen, J.W.; et al. Advanced smart tungsten alloys for a future fusion power plant. *Plasma Phys. Control. Fusion* **2017**, *59*, 064003. [CrossRef]
10. Calvo, A.; García-Rosales, C.; Koch, F.; Ordas, N.; Iturriza, I.; Greuner, H.; Pintsuk, G.; Sarbu, C. Manufacturing and testing of self-passivating tungsten alloys of different composition. *Nucl. Mater. Energy* **2016**, *9*, 422–429. [CrossRef]
11. Litnovsky, A.; Wegener, T.; Klein, F.; Linsmeier, C.; Rasinski, M.; Kreter, A.; Tan, X.; Schmitz, J.; Coenen, J.W.; Mao, Y.; et al. New oxidation-resistant tungsten alloys for use in the nuclear fusion reactors. *Phys. Scr.* **2017**, *T170*, 014012. [CrossRef]
12. Litnovsky, A.; Schmitz, J.; Klein, F.; De Lannoye, K.; Weckauf, S.; Kreter, A.; Rasinski, M.; Coenen, J.W.; Linsmeier, C.; Gonzalez-Julian, J.; et al. Smart Tungsten-based Alloys for a First Wall of DEMO. *Fusion Eng. Des.* **2020**, *159*, 111742. [CrossRef]
13. Coenen, J.W. Fusion Materials Development at Forschungszentrum Jülich. *Adv. Eng. Mater.* **2020**, *22*, 1–15. [CrossRef]
14. Mevrel, R. Cyclic oxidation of high-temperature alloys. *Mater. Sci. Technol.* **1987**, *3*, 531–535. [CrossRef]
15. Przybylski, K.; Garratt-Reed, A.J.; Yurek, G.J. Grain Boundary Segregation of Yttrium in Chromia Scales. *J. Electrochem. Soc.* **1988**, *135*, 509–517. [CrossRef]
16. *The Role of Active Elements in the Oxidation Behaviour of High Temperature Metals and Alloys*; Springer Science and Business Media LLC.: Berlin, Germany, 1989.
17. Stroosnijder, M.; Sunderkötter, J.; Cristóbal, M.J.; Jenett, H.; Isenbügel, K.; Baker, M. The influence of yttrium ion implantation on the oxidation behaviour of powder metallurgically produced chromium. *Surf. Coat. Technol.* **1996**, *83*, 205–211. [CrossRef]
18. Birks, N.; Meier, G.H.; Pettit, F.S. *Introduction to the High-Temperature Oxidation of Metals*, 2nd ed.; Cambridge University Press: Cambridge, UK, 2006.
19. Koch, F.; Köppl, S.; Bolt, H. Self Passivating W-Based Alloys as Plasma-Facing Material. *J. Nucl. Mater.* **2009**, *386–388*, 572–574. [CrossRef]
20. Koch, F.; Brinkmann, J.; Lindig, S.; Mishra, I.T.P.; Linsmeier, C. Oxidation behaviour of silicon-free tungsten alloys for use as the first wall material. *Phys. Scr.* **2011**, *T145*, 014019. [CrossRef]
21. Wegener, T.; Klein, F.; Litnovsky, A.; Rasinski, M.; Brinkmann, J.; Koch, F.; Linsmeier, C. Development and analyses of self-passivating tungsten alloys for DEMO accidental conditions. *Fusion Eng. Des.* **2017**, *124*, 183–186. [CrossRef]
22. Telu, S.; Mitra, R.; Pabi, S.K. Effect of Y_2O_3 Addition on Oxidation Behavior of W-Cr Alloys. *Met. Mater. Trans. A* **2015**, *46*, 5909–5919. [CrossRef]
23. Pilling, N.B.; Bedworth, R.E. The Oxidation of Metals at High Temperatures. *J. Instit. Meter.* **1923**, *29*, 529.
24. López-Ruiz, P.; Ordas, N.; Lindig, S.; Koch, F.; Iturriza, I.; García-Rosales, C. Self-passivating bulk tungsten-based alloys manufactured by powder metallurgy. *Phys. Scr.* **2011**, *T145*, 014018. [CrossRef]
25. Calvo, A.; García-Rosales, C.; Ordás, N.; Iturriza, I.; Schlueter, K.; Koch, F.; Pintsuk, G.; Tejado, E.; Pastor, J.Y. Self-passivating W-Cr-Y alloys: Characterization and testing. *Fusion Eng. Des.* **2017**, *124*, 1118–1121. [CrossRef]
26. Sal, E.; García-Rosales, C.; Schlueter, K.; Hunger, K.; Gago, M.; Wirtz, M.; Calvo, A.; Andueza, I.; Neu, R.; Pintsuk, G. Microstructure, oxidation behaviour and thermal shock resistance of self-passivating W-Cr-Y-Zr alloys. *Nucl. Mater. Energy* **2020**, *24*, 100770. [CrossRef]
27. Klein, F.; Wegener, T.; Litnovsky, A.; Rasinski, M.; Tan, X.; Gonzalez-Julian, J.; Schmitz, J.; Bram, M.; Coenen, J.; Linsmeier, C. Oxidation resistance of bulk plasma-facing tungsten alloys. *Nucl. Mater. Energy* **2018**, *15*, 226–231. [CrossRef]
28. Tan, X.; Klein, F.; Litnovsky, A.; Wegener, T.; Schmitz, J.; Linsmeier, C.; Coenen, J.; Breuer, U.; Rasinski, M.; Li, P.; et al. Evaluation of the high temperature oxidation of W-Cr-Zr self-passivating alloys. *Corros. Sci.* **2019**, *147*, 201–211. [CrossRef]
29. García-Rosales, C.; López-Ruiz, P.; Alvarez-Martín, S.; Calvo, A.; Ordas, N.; Koch, F.; Brinkmann, J. Oxidation behaviour of bulk W-Cr-Ti alloys prepared by mechanical alloying and HIPing. *Fusion Eng. Des.* **2014**, *89*, 1611–1616. [CrossRef]

30. Klein, F.; Litnovsky, A.; Wegener, T.; Tan, X.; Gonzalez-Julian, J.; Rasinski, M.; Schmitz, J.; Linsmeier, C.; Bram, M.; Coenen, J.W. Sublimation of advanced tungsten alloys under DEMO relevant accidental conditions. *Fusion Eng. Des.* **2019**, *146*, 1198–1202. [CrossRef]
31. Klein, F. Oxidation Resistant Tungsten Alloys Improving the Safety of Future Fusion Power Plants. Ph.D. Thesis, Ruhr-University, Bochum, Germany, 2019.
32. Litnovsky, A.; Wegener, T.; Klein, F.; Linsmeier, C.; Rasinski, M.; Kreter, A.; Unterberg, B.; Vogel, M.; Kraus, S.; Breuer, U.; et al. Smart alloys for a future fusion power plant: First studies under stationary plasma load and in accidental conditions. *Nucl. Mater. Energy* **2017**, *12*, 1363. [CrossRef]
33. Schmitz, J.; Litnovsky, A.; Klein, F.; Wegener, T.; Tan, X.; Rasinski, M.; Mutzke, A.; Hansen, P.; Kreter, A.; Pospieszczyk, A.; et al. WCrY smart alloys as advanced plasma-facing materials—Exposure to steady-state pure deuterium plasmas in PSI-2. *Nucl. Mater. Energy* **2018**, *15*, 220–225. [CrossRef]
34. Schmitz, J.; Litnovsky, A.M.; Klein, F.; Tan, X.; Breuer, U.; Rasinski, M.; Ertmer, S.; Kreter, A.; Gonzalez-Julian, J.; Bram, M.; et al. Argon-seeded plasma exposure and oxidation performance of tungsten-chromium-yttrium smart alloys. *Tungsten* **2019**, *1*, 159–168. [CrossRef]
35. Schmitz, J.; Litnovsky, A.; Klein, F.; De Lannoye, K.; Kreter, A.; Rasinski, M.; Breuer, U.; Gonzalez-Julian, J.; Bram, M.; Coenen, J.W.; et al. On the plasma suitability of WCrY smart alloys—The effect of mixed D+Ar/He plasmas. *Phys. Scr.* **2020**, *T171*, 014002. [CrossRef]
36. Schmitz, J. Development of Tungsten Alloy Plasma-Facing Materials for the Fusion Power Plant. Ph.D. Thesis, Ghent University and University of Bochum, Bochum, Germany, 2020.
37. Schmitz, J.; Mutzke, A.; Litnovsky, A.; Klein, F.; Tan, X.; Wegener, T.; Hansen, P.; Aghdassi, N.; Eksaeva, A.; Rasinski, M.; et al. Preferential sputtering induced Cr-Diffusion during plasma exposure of WCrY smart alloys. *J. Nucl. Mater.* **2019**, *526*, 151767. [CrossRef]
38. Barabash, V. *Material Specification for the Supply of Tungsten Bars for the ITER Divertor*; ITER Document ITER_D_2X38PN; ITER Organization: Saint-Pole-du-Lonque, France, 2010; pp. 1–7.
39. Barabash, V. *Material Specification for the Supply of Tungsten Plates for the ITER Divertor*; ITER Document No. ITER_D_2EDZJ4; ITER Organization: Saint-Pole-du-Lonque, France, 2009; pp. 1–7.
40. Igitkhanov, Y.; Bazylev, B.; Landman, I.; Fetzer, R. *Design Strategy for the PFC in DEMO Reactor (KIT Scientific Reports; 7637)*; European Geosciences Union (EGU): Munich, Germany, 2013.
41. Tokar, M.Z. An assessment for the erosion rate of DEMO first wall. *Nucl. Fusion* **2018**, *58*, 016016. [CrossRef]
42. Federici, G.; Biel, W.; Gilbert, M.R.; Kemp, R.; Taylor, N.; Wenninger, R. European DEMO design strategy and consequences for materials. *Nucl. Fusion* **2017**, *57*, 092002. [CrossRef]
43. Wang, W.; Tan, X.; Liu, J.; Chen, X.; Wu, M.; Luo, L.; Zhu, X.; Chen, H.; Mao, Y.; Litnovsky, A.; et al. The influence of heating rate on W-Cr-Zr alloy densification process and microstructure evolution during spark plasma sintering. *Powder Technol.* **2020**, *370*, 9–18. [CrossRef]
44. Wang, W.; Tan, X.; Yang, S.; Luo, L.; Zhu, X.; Mao, Y.; Litnovsky, A.; Coenen, J.; Linsmeier, C.; Wu, Y. On grain growth and phase precipitation behaviors during W-Cr-Zr alloy densification using field-assisted sintering technology. *Int. J. Refract. Met. Hard Mater.* **2021**, *98*, 105552. [CrossRef]
45. Mitteau, R.; Stangeby, P.; Lowry, C.; Merola, M. Heat loads and shape design of the ITER first wall. *Fusion Eng. Des.* **2010**, *85*, 2049–2053. [CrossRef]
46. Mitteau, R.; Calcagno, B.; Chappuis, P.; Eaton, R.; Gicquel, S.; Chen, J.; Labusov, A.; Martin, A.; Merola, M.; Raffray, R.; et al. The design of the ITER first wall panels. *Fusion Eng. Des.* **2013**, *88*, 568–570. [CrossRef]
47. Gusev, V.G.; Sobol'Kov, A.V.; Aborkin, A.V.; Alymov, M.I. Simulation of the Energy–Force Parameters of Planetary Ball Mill Processing and Estimation of Their Influence on the Particle Size in an AMg2 Alloy/Graphite Composite Powder. *Russ. Met. (Metally)* **2019**, *2019*, 24–30. [CrossRef]
48. Litunovsky, N.; Alekseenko, E.; Makhankov, A.; Mazul, I. Development of the armoring technique for ITER Divertor Dome. *Fusion Eng. Des.* **2011**, *86*, 1749–1752. [CrossRef]
49. Gervash, A.; Giniyatulin, R.; Guryeva, T.; Glazunov, D.; Kuznetsov, V.; Mazul, I.; Ogursky; Piskarev, P.; Safronov, V.; Eaton, R.; et al. The development of technology of Be/CuCrZr joining using induction brazing. *Fusion Eng. Des.* **2019**, *146*, 2292–2296. [CrossRef]
50. Sal, E.; de Prado, J.; Sánchez, M.; Ureña, A.; García-Rosales, C. Joining of self-passivating W-Cr-Y alloy to ferritic-martensitic steel by hot isostatic pressing. *Fusion Eng. Des.* **2021**, *170*, 112499. [CrossRef]
51. de Prado, J.; Sánchez, M.; Calvo, A.; García-Rosales, C.; Ureña, A. Development of self passivating W-Eurofer brazed joints. *Fusion Eng. Des.* **2019**, *146*, 1810–1813. [CrossRef]
52. de Prado, J.; Sánchez, M.; Antusch, S.; Ureña, A. Development of W-composites/EUROFER brazed joints for the first wall component of future fusion reactors. *Phys. Scr.* **2017**, *T170*, 014026. [CrossRef]
53. Bachurina, D.; Suchkov, A.; Kalin, B.; Sevriukov, O.; Fedotov, I.; Dzhumaev, P.; Ivannikov, A.; Leont'Eva-Smirnova, M.; Mozhanov, E. Joining of Tungsten with Low-Activation Ferritic–Martensitic Steel and Vanadium Alloys for Demo Reactor. *Nucl. Mater. Energy* **2018**, *15*, 135–142. [CrossRef]

54. Bachurina, D.; Tan, X.-Y.; Klein, F.; Suchkov, A.; Litnovsky, A.; Schmitz, J.; Gonzalez-Julian, J.; Bram, M.; Coenen, J.W.; Wu, Y.-C.; et al. Self-passivating smart tungsten alloys for DEMO: A progress in joining and upscale for a first wall mockup. *Tungsten* **2021**, *3*, 101–115. [CrossRef]
55. Guillon, O.; Gonzalez-Julian, J.; Dargatz, B.; Kessel, T.; Schierning, G.; Räthel, J.; Herrmann, M. Field-Assisted Sintering Technology/Spark Plasma Sintering: Mechanisms, Materials, and Technology Developments. *Adv. Eng. Mater.* **2014**, *16*, 830–849. [CrossRef]
56. Bram, M.; Laptev, A.M.; Mishra, T.P.; Nur, K.; Kindelmann, M.; Ihrig, M.; Da Silva, J.G.P.; Steinert, R.; Buchkremer, H.P.; Litnovsky, A.; et al. Application of Electric Current-Assisted Sintering Techniques for the Processing of Advanced Materials. *Adv. Eng. Mater.* **2020**, *22*, 2000051. [CrossRef]
57. Klein, F.; Litnovsky, A.; Tan, X.; Gonzalez-Julian, J.; Rasinski, M.; Linsmeier, C.; Bram, M.; Coenen, J.W. Smart alloys as armor material for DEMO: Overview of properties and joining to structural materials. *Fusion Eng. Des.* **2021**, *166*, 112272. [CrossRef]
58. Sobieraj, D.; Wróbel, J.S.; Gilbert, M.R.; Litnovsky, A.; Klein, F.; Kurzydłowski, K.J.; Nguyen-Manh, D. Composition Stability and Cr-Rich Phase Formation in W-Cr-Y and W-Cr-Ti Smart Alloys. *Metals (Basel)* **2021**, *11*, 743. [CrossRef]
59. Wróbel, J.S.; Nguyen-Manh, D.; Kurzydlowski, K.J. Ab Initio Based Modelling of Diffusion and Phase Stability of Alloys. *Diffus. Found.* **2017**, *12*, 1–22. [CrossRef]
60. Nguyen-Manh, D.; Lavrentiev, M.Y.; Muzyk, M.; Dudarev, S.L. First-principles models for phase stability and radiation defects in structural materials for future fusion power-plant applications. *J. Mater. Sci.* **2012**, *47*, 7385–7398. [CrossRef]
61. Nguyen-Manh, D. Ab-Initio Modelling of Point Defect-Impurity Interaction in Tungsten and other BCC Transition Metals. *Adv. Mater. Res.* **2008**, *59*, 253–256. [CrossRef]
62. Kresse, G.; Furthmüller, J. Efficiency of ab-initio total energy calculations for metals and semiconductors using a plane-wave basis set. *Comput. Mater. Sci.* **1996**, *6*, 15–50. [CrossRef]
63. Kresse, G.; Furthmüller, J. Efficient iterative schemes forab initiototal-energy calculations using a plane-wave basis set. *Phys. Rev. B* **1996**, *54*, 11169–11186. [CrossRef]
64. van de Walle, A.; Asta, M.; Ceder, G. The alloy theoretic automated toolkit: A user guide. *Calphad* **2002**, *26*, 539–553. [CrossRef]
65. Nguyen-Manh, D.; Wróbel, J.S.; Klimenkov, M.; Lloyd, M.J.; Messina, L.; Dudarev, S.L. First-principles model for voids decorated by transmutation solutes: Short-range order effects and application to neutron irradiated tungsten. *Phys. Rev. Mater.* **2021**, *5*, 065401. [CrossRef]
66. Warren, B.E. *X-ray Diffraction*; Dover Publications: New York, NY, USA, 1990.
67. Cowley, J.M. An Approximate Theory of Order in Alloys. *Phys. Rev.* **1950**, *77*, 669–675. [CrossRef]
68. Massalski, T.; Submanian, P.; Okamoto, H. *Binary Alloy Phase Diagrams*, 2nd ed.; Baker, H., Okamoto, H., Eds.; ASM International: Amir, The Netherlands, 1998; Volume 3.
69. Gilbert, M.R.; Arakawa, K.; Bergstrom, Z.; Caturla, M.; Dudarev, S.; Gao, F.; Goryaeva, A.; Hu, S.; Hu, X.; Kurtz, R.; et al. Perspectives on multiscale modelling and experiments to accelerate materials development for fusion. *J. Nucl. Mater.* **2021**, *554*, 153113. [CrossRef]
70. Klein, F.; Wegener, T.; Litnovsky, A.; Rasinski, M.; Tan, X.; Schmitz, J.; Linsmeier, C.; Coenen, J.W.; Du, H.; Mayer, J.; et al. On Oxidation Resistance Mechanisms at 1273 K of Tungsten-Based Alloys Containing Chromium and Yttria. *Metals (Basel)* **2018**, *8*, 488. [CrossRef]
71. Mutzke, A.; Schneider, R.; Eckstein, W.; Dohmen, R.; Schmid, K.; von Toussaint, U.; Badelow, G. *SDTrimSP Version 6.00*; Max-Planck-Institut für Plasmaphysik: Garching, Germany, 2019.
72. Ricapito, I.; Ciampichetti, A.; Benamati, G. Pb–17Li/water interaction in DEMO WCLL blanket: Water micro-leaks. *Fusion Eng. Des.* **2003**, *65*, 577–587. [CrossRef]
73. Wu, Y.; Chen, Z.; Hu, L.; Jin, M.; Li, Y.; Jiang, J.; Yu, J.; Alejaldre, C.; Stevens, E.; Kim, K.; et al. Identification of safety gaps for fusion demonstration reactors. *Nat. Energy* **2016**, *1*, 16154. [CrossRef]
74. Kurnaev, V.; Afonin, O.; Antipenkov, A.; Koborov, N.; Mukhammedzyanov, T.; Ochkin, V.; Pearce, R.; Pleshkov, E.; Podolyako, F.; Sorokin, I.; et al. Spectroscopic localization of water leaks in iter. *Fusion Eng. Des.* **2013**, *88*, 1414–1417. [CrossRef]
75. Antipenkov, A.B.; Afonin, O.N. On the problem of water microleak detection in the tokamak chamber. *Bull. Lebedev Phys. Inst.* **2010**, *37*, 291–295. [CrossRef]